ADVANCED FUNCTIONAL MATERIALS
www.afm-journal.de

Oxygen-Free Highly Conductive Graphene Papers

Petr Šimek, Zdeněk Sofer, Ondřej Jankovský, David Sedmidubský, and Martin Pumera**

Graphene papers have a potential to overcome the gap from nanoscale graphene to real macroscale applications of graphene. A unique process for preparation of highly conductive graphene thin paper by means of Ar^+ ion irradiation of graphene oxide (GO) papers, with carbon/oxygen ratio reduced to 100:1, is presented. The composition of graphene paper in terms of carbon/oxygen ratio and in terms of types of individual oxygen-containing groups is monitored throughout the process. Angle-resolved high resolution X-ray photoelectron spectroscopy helps to investigate the depth profile of carbon and oxygen within reduced GO paper. C/O ratios over 100 on the surface and 40 in bulk material are observed. In order to bring insight to the processes of oxygen removal from GO paper by low energy Ar^+ ion bombardment, the gases released during the irradiation are analyzed by mass spectroscopy. It is proven that Ar^+ ion beam can be applied as a technique for fabrication of highly reduced graphene papers with high conductivities. Such highly conductive graphene papers have great potential to be used in application for construction of microelectronic and sensor devices.

1. Introduction

Graphene or GO papers attract attention for their interesting properties and possible uses such as antibacterial paper and part of anodes of Li ion batteries.[1–6] GO paper-like materials (or foils) had shown improved properties over other paper-like materials. It outperforms other paper materials namely in stiffness and strength. Since their first synthesis by vacuum filtration of colloidal dispersions of graphene oxide sheets through an Anodisc membrane filter in 2007,[7] many other methods for the synthesis of graphene based papers from GO sheets have been developed.[8–10] For example, self-assembly of GO membranes by evaporating the hydrosol also yielded foils with good mechanical properties.[11] The mechanical properties of GO foils can be further enhanced by modification with small amount of divalent ions bonded to the functional groups on GO sheets. The divalent ion serves as a cross-linking element between two neighboring carboxyl groups of the GO sheets. The divalent alkali metals (Mg^{2+}, Ca^{2+}) are ideal choice for such purpose.[12] For example, on nanometer scale, few nanometers thin GO foils were prepared by a modified spin-coating method and used to fabricate radio frequency resonators with high quality factors and figures of merit exceeding those of pure graphene layers.[13,14] Cross-linking the GO sheets already in dispersion and subsequently evaporating the solvent to make cross-linked GO papers represents an alternative approach.[15] The typical carbon/oxygen ratio of such papers ranges from 1.2 to 2.7.[11–15]

GO papers exhibit poor electrical conductivity and therefore their applications in electronic devices are limited. This obstacle could be overcome by a fabrication of graphene paper (i.e., reduced GO papers). However, it is problematic to produce such paper from graphene dispersion due to its non-polar character. Several solutions to this problem were sought, such as thermal annealing the GO foils in various atmospheres,[16] or using surfactant stabilizers to make water-dispersible graphene sheets.[17] Some reports suggest the same procedure for chemically reduced GO (with hydrazine) as for GO foils, with consequent annealing of the resulting graphene paper.[7,18] Another reported method is a reaction of GO dispersion with potassium hydroxide and subsequent reaction with hydrazine which yielded water-dispersible graphene sheets that were then turned into electrically conductive graphene paper.[19] Hexylamine functionalization and subsequent reaction of wet GO paper with hydrazine also yielded electrically conductive graphene paper.[20] Carbon/oxygen ratios of graphene papers were typically in the range of 2.6 to 14.1.[16–20]

We suggest a simple method for preparation of highly conductive papers which avoids solution chemistry based reduction and yields a uniquely high C/O ratio and electrical conductivity of the resulting graphene paper. In our work, we employed Ar^+ ion irradiation of GO oxide papers as a reduction step. Highly dense, highly conductive and chemically stable graphene paper material offers large application potential for development of new microelectronic devices, solar cells and electrochemical power sources.

P. Šimek, Dr. Z. Sofer, O. Jankovský,
Prof. D. Sedmidubský
Department of Inorganic Chemistry
Institute of Chemical Technology
Technická 5, Prague 6
166 28, Czech Republic
E-mail: zdenek.sofer@vscht.cz
Dr. M. Pumera
Division of Chemistry & Biological Chemistry
School of Physical and Mathematical Sciences
Nanyang Technological University
Singapore 637371, Singapore
E-mail: pumera@ntu.edu.sg

DOI: 10.1002/adfm.201304284

Figure 1. Photograph of the prepared graphene paper.

2. Results and Discussion

We prepared graphene oxide by modified Hummers method and consequently synthesized GO paper by vacuum drying of GO water dispersion on stainless steel plate (see **Figure 1**). The resulting GO paper was exposed to Ar^+ ion irradiation which reduced the graphene oxide to graphene with extremely high C/O ratio. This process is shown in **Scheme 1**. Graphite oxide and graphene papers were studied by high resolution and angle resolved X-ray photoelectron spectroscopy in situ during argon ion irradiation of the GO surface. We investigated the composition of gas evolved during the irradiation by the quadrupole mass spectrometer connected directly to the XPS measurement chamber to gain insight into the processes occurring during the reduction.

The surface was further characterized by atomic force microscopy and scanning electron microscopy. Electrical resistivity mapping was determined by AFM in scanning spreading resistance mode. The prepared graphene paper exhibits high electrical conductivity and C/O ratio over 100 with oxygen free surface of reduced GO paper. We studied the effect of irradiation of GO paper by Ar^+ beam with energies of 1.0, 2.5 and 5 keV. The results are described and discussed below.

The surface of GO paper was irradiated with Ar plasma of energy 1 keV to deoxygenate the GO paper. Angle resolved XPS was performed perpendicularly (labeled "BULK" in the further discussion) and under 10° angle (label "SURF") to the surface in order to investigate surface properties of GO at various steps of irradiation. The low angle XPS measurement provides information about the composition of the first atomic layer on the surface. The perpendicular X-ray irradiation gives information about composition from depths up to ten nanometers. XPS spectra were recorded several times, 0 s (prior to irradiation), 15 s, 45 s, 3 min, 5 min, and 20 min after irradiation. The XPS survey spectra at 0 s and 20 min are presented in **Figure 2**A,B. The C 1s and O 1s peaks are clearly visible, energy maxima of these peaks are at ≈285 eV and ≈533 eV. The C/O ratio for both scans was calculated based on the C 1s and O 1s peak areas. Figure 2C shows the C/O ratio as a function of time. It is obvious that the C/O ratio is increasing with the duration of the irradiation. However, the energy of 1 keV is not sufficient to reach a full reduction and a removal of all the oxygen containing groups in the structure. The C/O ratio increased from ≈3 to ≈12 in BULK and from ≈4 to ≈18 in SURF, respectively. We can conclude from this finding that for such low energies most of the Ar^+ ions are stopped in the first few atomic layers of the surface where their energy is dissipated. The material in the depths of about 10 nm remains almost unchanged. Based on the simulation using SRIM software, the stopping range of Ar^+ ions in graphite oxide is about 4 nm with longitudinal struggling of about 1.5 nm. This value is far lower compared to information obtained from XPS in the perpendicular configuration.

Detailed high resolution XPS spectra of C 1s (Figure S1, Supporting Information) show the process of reduction before irradiation – 0 min and 3 min, 5 min and 20 min during irradiation. At the beginning, a second peak at ≈287 eV which is associated with the oxygen containing groups is noticeable. The intensity of this peak distinctly decreases with increasing time of irradiation and this peak entirely disappears at 20 min. Only a single peak with an asymmetrical tail at higher energies remains. O 1s peak is shown in Figure S1, Supporting Information. Lower intensities are connected to the successful reduction of the GO paper.

Careful curve fitting was performed on the C 1s (see Figure S2, Supporting Information) spectrum to quantitatively differentiate the six different carbon stages in the sample: the C–C (≈284.5 eV), the C–C/C–H (≈285.6 eV), the C–O of alcohol/ether groups (≈286.6 eV), the C = O of carbonyl groups (287.5 eV), –C = O of carboxyl/ester groups (289.9 eV) and the π–π^* interaction (291.2 eV). Results of the fitting are shown in **Table 1** where the composition of each functional group in BULK and SURF measurements is compared. It is evident that there is a significant reduction of the oxygen containing functional groups. Very unusual is a big increase of the C–C bonded carbon on the surface of reduced

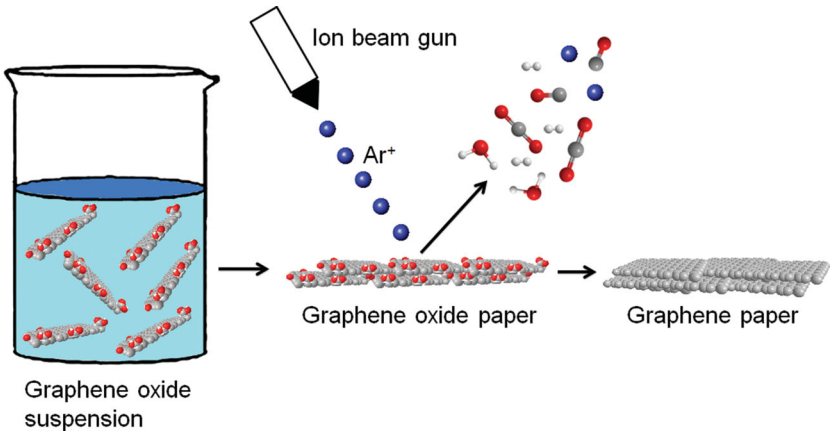

Scheme 1. Preparation of the graphene paper by Ar^+ ion irradiation.

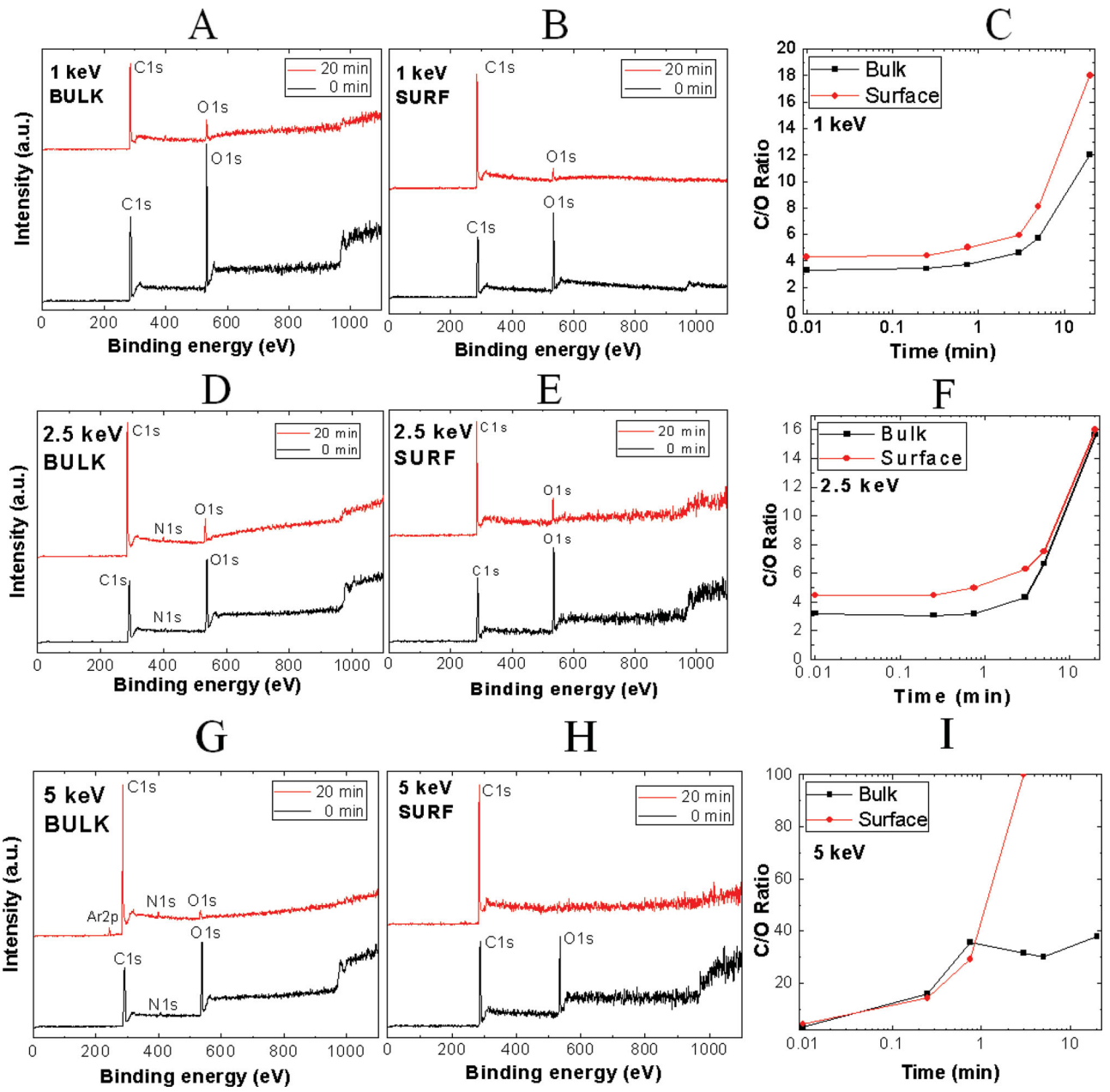

Figure 2. A,D,G) Survey BULK XPS spectra of GO papers before and after 20 min of Ar^+ ion irradiation for 1, 2.5, and 5 keV, respectively. B,E,H) Survey SURF XPS spectra of GO papers before and after 20 min of Ar^+ ion irradiation for 1, 2.5, and 5 keV, respectively. C,F,I) C/O SURF and BULK ratios of the graphene papers as determined by XPS for 1, 2.5, and 5 keV, respectively.

GO. This led us to a conclusion that reduced graphene on the surface most probably reacts with byproducts of GO reduction in the depth of the material and partially hydrogenated graphene is formed on the surface.

A similar approach was performed with Ar^+ ion beam with energy of 2.5 keV. The survey spectra before irradiation and after 20 min of irradiation are compared in Figure 2D and Figure 2E. There are C 1s and O 1s peaks in the spectrum of the SURF measurement, while in the BULK spectrum there is a third peak at ≈399 eV apart from the C 1s and O 1s peaks. This peak belongs to traces of N 1s and it is present due to impurities from the GO paper synthesis. The dependence of C/O ratio on time is plotted in Figure 2F. The C/O ratio is increasing similarly to the case of irradiation with ions of energy 1 keV. Neither 2.5 keV nor 1 keV is sufficient for the total reduction. The C/O ratio increased from ≈3 to ≈16 in BULK and from ≈4 to ≈16 in SURF. Minimal differences in the C/O ratio on surface and in the bulk of the material indicate sufficient energy of Ar^+ ions to penetrate into the depth corresponding to the XPS measurements. This was also confirmed by the simulation using SRIM software when the projected range of Ar^+ ions was 7.5 nm and the longitudinal struggling 2.5 nm. The increased degree of reduction and its depth was also confirmed by the spreading resistance microscopy.

Table 1. BULK and SURF functional group composition of irradiated graphene papers, energy of Ar^+ ion beam 1 keV.

	C = C [%]	C–C/C–H [%]	C–O [%]	C = O [%]	O–C = O [%]	π–π^* [%]
BULK Time [min]						
0	36.76	13.68	25.91	23.26	0.14	0.25
3	31.07	21.51	24.39	8.46	13.21	1.37
5	43.39	22.27	14.15	9.76	4.82	5.62
20	53.02	17.16	9.59	11.95	4.71	3.25
SURF Time [min]						
0	34.83	23.24	23.44	13.40	2.60	2.48
3	51.91	29.17	18.91	11.62	7.63	3.68
5	47.77	31.01	12.96	7.21	4.37	3.89
20	51.66	48.34	7.93	7.93	6.79	6.94

The C 1s high resolution XPS spectra for BULK and SURF are shown in Figure S3 (Supporting Information) at 0, 3, 5, and 20 min of Ar^+ irradiation. It is noticeable that the amount of oxygen containing groups (second peak at ≈287 eV) is reduced faster than in the case of lower ion energy. The O 1 s peak is shown in Figure S3 for BULK and SURF, respectively. Also in this case, it is possible to observe a successful reduction of GO foil. The highest differences in composition are observed in the first 5 min, whereas further irradiation led only to a slight improvement compared to the sample irradiated for 5 minutes.

Careful curve fitting was also performed on the C 1s peak of BULK and of SURF (Figure S4, Supporting Information) with the resulting representation of individual groups: C–C, C–C and C–H, C–O, C = O, O–C = O, and π–π^* interaction. The results of the fitting are shown in **Table 2**. While the amount of C = C and C–C groups is increasing, the amount of oxygen containing groups is essentially suppressed. However, some unusual behavior is detected. Surprisingly we can observe a concentration increase of groups corresponding to the carboxylic acid and the π–π^* interaction. The origin of this effect is not clear and most probably results from the interaction of graphene with complex organic molecules evolved from graphite oxide during irradiation. The formed organic molecules can interact with graphene and remain non-covalently bonded within the reduced graphene foil.

The last and highest energy of Ar^+ ions used for GO paper reduction was set to 5 keV. The survey spectra prior to irradiation and after 20 min of irradiation are compared in Figure 2G and Figure 2H. Apart from the C 1s and O 1s peaks, the N 1s peak at 399 eV and Ar 2p peak at ~242 eV are also present in the BULK sample after irradiation. The theoretical projected range of Ar^+ ions in GO is about 11 nm with longitudinal struggling of 3.5 nm. Fur such energy other effects like argon implantation between the layers of GO layer or sputtering effects can be anticipated. Sputtering is well documented by the observation of hydrocarbon radicals in the mass spectra. The sputtering effects are also documented by the XPS spectra where there were no significant changes in the C/O ratio after 5 min of treatment. The energy of 5 keV is sufficient for the reduction of GO foil surface, therefore the O 1s peak shows a minimum intensity in survey spectra and completely disappears from the surface of irradiated GO paper (Figure 2H). The irradiation time dependence of the C/O ratio is plotted in Figure 2I. GO paper becomes fully reduced after 3 min, the C/O ratio in BULK then remains constant at ≈35 and in SURF becomes higher than 100. Such high C/O ratio is very unusual and the concentration of oxygen on the surface was below the detection limit of XPS (which is about 0.1 at %). The extremely high degree of reduction is also documented by the conductivity measurements on the surface of graphene papers.

The C 1s high resolution XPS spectra are shown in Figure S5 (Supporting Information) at 0 s, 15 s, 45 s, and 3 min of Ar^+ irradiation. An extremely fast reduction of the material can be deduced from these figures. Figure S6 (Supporting Information) shows the analysis of the C 1s peak for BULK and SURF. The results of the fitting are summarized in **Table 3**. These results indicate that the process of Ar^+ irradiation with energy of 5 keV is an effective route for the synthesis of highly reduced conductive graphene foils.

The morphology of GO papers before the reduction is shown in Figure S7, Supporting Information. Microscope images of paper after the irradiation with Ar^+ ions of various energies are shown in Figure S8A, Supporting Information. The SEM

Table 2. BULK and SURF functional group composition of irradiated graphene papers, energy of Ar^+ ion beam 2.5 keV.

	C = C [%]	C–C/C–H [%]	C–O [%]	C = O [%]	O–C = O [%]	π–π^* [%]
BULK Time [min]						
0	37.17	9.92	39.80	8.42	0.89	3.81
3	48.00	9.61	23.41	7.88	8.05	3.05
5	44.15	18.17	17.18	6.90	9.62	3.98
20	53.36	12.69	16.72	4.37	7.04	5.82
SURF Time [min]						
0	34.77	7.17	40.42	14.19	1.80	1.65
3	61.55	14.68	13.85	5.23	0.97	3.72
5	60.23	15.73	11.05	5.37	3.58	4.02
20	56.97	18.34	10.60	4.13	4.26	5.69

Table 3. BULK and SURF functional group composition of irradiated graphene papers, energy of Ar^+ ion beam 5 keV.

	C = C [%]	C–C/C–H [%]	C–O [%]	C = O [%]	O–C = O [%]	π–π^* [%]
BULK Time [min]						
0	59.01	12.67	22.83	4.03	0.99	0.47
3	48.49	21.38	13.22	6.24	4.57	6.10
5	41.50	35.87	9.18	4.22	3.61	5.62
20	56.81	13.36	14.63	4.95	7.40	2.85
SURF Time [min]						
0	38.37	12.67	39.58	5.29	2.76	1.33
3	61.93	16.98	8.08	5.41	4.44	3.15
5	60.66	19.27	6.25	6.35	2.80	4.68
20	51.13	14.92	18.08	8.16	3.67	4.04

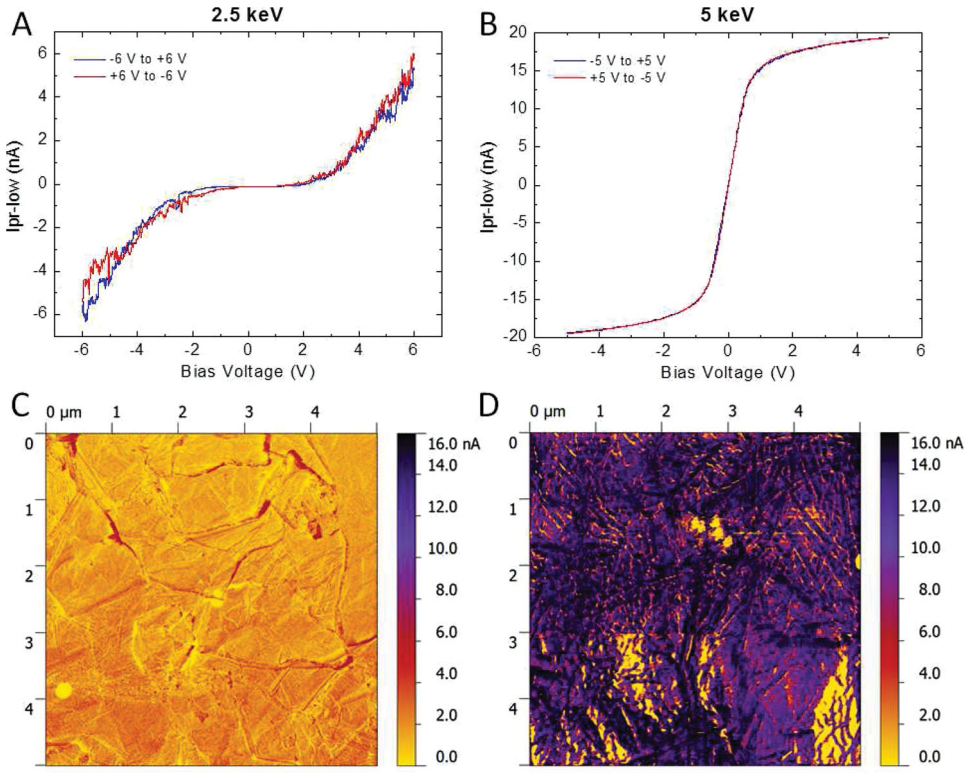

Figure 3. A,B) Examples of *I–V* curves measured on the graphene paper surface for 2.5 keV and 5 keV, respectively. C,D) Corresponding conductivity maps for 2.5 keV and 5 keV, respectively. Conductivity maps were acquired using bias voltage of 5 V.

pictures were acquired from surfaces irradiated for 20 min. The typical lamellar structure with wrinkled sheets of GO can be observed. No significant changes in the morphology can be observed after the Ar^+ ion beam irradiation. This is caused by narrow thickness of graphene formed by the reduction of the GO paper surface. Only a minimum porosity and a compact structure of the papers can be observed. The reduction by low energy ion beam does not cause any significant morphology or structure changes.

AFM techniques were used to document other properties of graphene paper. We examined the morphology of GO papers by atomic force microscopy (AFM) and the conductivity by spreading resistance microscopy (SSRM). The surface morphology of GO foils prior to the irradiation and after the treatment with ions of various energies is shown in Figure S8B, Supporting Information. No significant changes were observed and all samples exhibited almost identical morphology. This is related to the low stopping range of Ar^+ ions at such low energies and also to the relatively "rough" surface of the GO foils. The surface roughness of foils was in the range of tenths of nm with height steps up to 500 nm.

In addition to AFM scans we also performed the spreading resistivity mapping using conductive AFM tips (SSRM). In the case of 5 keV the irradiated sample was highly conductive. However, some shadow effects appeared on the surface. These effects are related to the construction and geometry of the Ar^+ ion gun which is positioned under the angle of 45° to the plane of sample surface. Under this configuration, some parts of the sample with rough surface can be screened and are thus not properly irradiated. In these places only minimal conductivity of the surface is measured. The surface image obtained on the 5 keV irradiated sample by AFM and SSRM is shown in **Figure 3**B. In the case of 1 keV the irradiation of the material preserves non-conductive properties typical for GO. For 2.5 keV we observed only a weak conductivity on minor areas of the surface (Figure 3A). In order to further analyze transport properties of the reduced GO surface, we performed the measurements of I/V curves. These measurements were done for samples irradiated with 2.5 and 5 keV and the results are shown in Figure 3C and 3D. The 2.5 keV sample shows a non-Ohmic behavior with a current threshold at about 2 V and only weak conductivity. The remaining oxygen functionalities are responsible for non-Ohmic semiconducting properties of sample surface. By contrast, the 5 keV irradiated samples show pure Ohmic contact behavior with the linear I/V dependence in the range of ±10 nA. The obtained I/V curve exhibits very high conductivity for 5 keV irradiated samples. Based on these results we can conclude that there is a significant dependence of the sample conductivity on the C/O ratio.

Surface resistivities of the reduced GO surfaces were determined by a standard four-probe technique. The 5 keV irradiated paper showed a sheet resistance of 70 kΩ sq^{-1}, while the 2.5 keV irradiated paper had a sheet resistance of 520 kΩ sq^{-1}. These values are comparable to some other graphene paper materials.[13] Sheet resistance of 1 keV irradiated GO paper was much higher, 750 MΩ sq^{-1}. Sheet resistance of GO paper was out of our measurement range (>1 GΩ sq^{-1}). Bulk conductivities of the reduced GO layers are experimentally hard

to evaluate because of the unknown exact thickness of the reduced layer. We can calculate bulk resistivities by multiplying the sheet resistance by the layer thickness. Bulk conductivity is then the inverse value of the bulk resistivity. In order to determine layer thickness, we assumed that the thickness of the irradiated layer is equal to the projected range of Ar^+ ions in graphite for given energies. For Ar^+ irradiation energies 1, 2.5,and 5 keV, the simulated projected ranges of Ar^+ ions are 4, 7.5, and 11 nm, respectively. The bulk conductivity of 5 keV irradiated layer is then 1300 S m^{-1}. For 2.5 keV irradiated layer we get 256 S m^{-1} and, finally, 0.3 S m^{-1} for 1 keV irradiated layer. If we compare these results with C/O ratios obtained from XPS, we will obtain increasing dependency of the electrical conductivity on the C/O ratio. For the C/O ratios of 12, 16, and 40, the bulk resistivities are 0.3, 256, and 1300 S m^{-1}, respectively.

To further demonstrate that reduction of the GO paper is localized only on the surface, we conducted measurements of mechanical strength, through plane thermal conductivity and thermal stability of GO and 5 keV irradiated samples. Thermogravimetric analysis and differential thermal analysis (Figure S10, Supporting Information) in dynamic air atmosphere were performed in order to determine weight loss and enthalpy change associated with thermal decomposition of the material at high temperatures. These properties are important for assessing the material's resistivity to increased temperatures. Two major effects can be observed. Between 220–240 °C weight loss of 30% for GO and 28% for 5 keV irradiated sample connected with an exothermic effect occurs. This is caused by decomposition of the oxygen containing functionalities from the paper.[16] Gradual weight loss continues until approximately 520 °C when burning of the graphene paper takes place. The maximum of this exothermic effect appears at 650 °C for both GO and 5 keV irradiated paper.

Through plane thermal conductivities of the GO paper and 5keV irradiated paper are 0.195 W mK^{-1} and 0.198 W mK^{-1}, respectively. Values of the thermal conductivity are much lower compared to graphite's thermal conductivity of 118.6 W mK^{-1}. Thermal diffusivities of GO (1.77×10^{-3} cm^2 s^{-1}) and 5 keV irradiated paper (1.80×10^{-3} cm^2 s^{-1}) are also lower compared to that of graphite (1.02 cm^2 s^{-1}). These findings support the assumption that GO sheets are ordered horizontally during the GO paper assembly. On the other hand, stacking in vertical direction causes worse heat transfer than in horizontal direction.

We compared tensile strength σ and Young's modulus E of GO and 5 keV irradiated papers. Both materials had similar tensile strength (64.7 ± 24.8 MPa and 63.0 ± 16.0 MPa for GO paper and 5 keV irradiated paper, respectively). Young's moduli of 9.0 ± 3.3 GPa for GO paper and 7.1 ± 1.4 GPa for 5 keV irradiated paper were calculated from the "linear region" of the stress–strain curves where the material undergoes elastic deformation. For example of a stress–strain curve, see Figure S11, Supporting Information.

The gas evolution was studied during the reduction of the GO paper caused by the irradiation by Ar^+ ions (for the energy of 5 keV). During the Ar^+ ions irradiation the increase of partial pressure of various species was observed. This is due to the reduction process which is accompanied by a removal of various oxygen functionalities from the surface. The evolution of gaseous species such as CO, CO_2, H_2O, and several complex organic molecules was reported during ion beam irradiation of GO under UHV conditions. The most significant increase of partial pressure was detected for the following atomic masses: 2 – H_2, 14 – N/CH_2^{2+}, 15 – CH_3, 16 – O/CH_4, 18 – H_2O, 28 – CO/N_2 and 44 – CO_2 which is noticeable from **Figure 4** (time dependence of partial pressure of various compounds). The partial pressure of neon (M = 20) was constant and unaffected by the sputtering (etching) of the surface. This signal corroborates the origin of evolved gases from GO – ion beam interaction. The hydrocarbons and their fractions (CH_4, CH_3^+) originate from the interaction of Ar^+ ions with GO and from

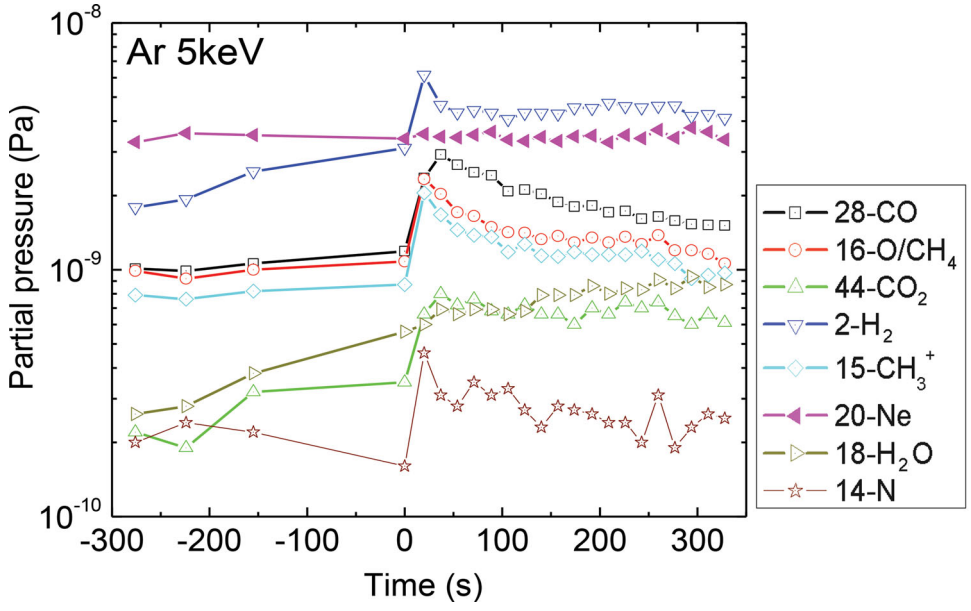

Figure 4. Partial pressure of species observed during irradiation with Ar^+ ions of energy 5 keV.

decomposition of oxygen functional groups. The other species are typical products of thermal exfoliation of GO (H_2O, CO, CO_2). The AMU 14 attributed to nitrogen can be also related to the hydrocarbon radical CH_2^{2+} which can exist at extremely low pressures in the measurement chamber (the mean free path of those particles is in the order of tenths of centimeters). The hydrogen molecules can be produced by the destruction of GO with high concentration of covalently bonded hydrogen containing functional groups (such as –OH and –COOH). Observation of hydrocarbon fragments indicates the ion beam induced etching of GO paper during irradiation procedure.

The Raman spectra of all irradiated samples are represented in Figure S9. Two most distinct peaks at ≈1350 cm^{-1} (D band) and ≈1600 cm^{-1} (G band) correspond to the defects in the hexagonal graphene lattice and to the graphitic frame lattice, respectively. The other two peaks at ≈2690 cm^{-1} and ≈2920 cm^{-1} belong to 2D and D'' bands, respectively. From the comparison of bands positions and their relative intensities we can conclude that the position of the bands is the same for all samples and relative intensities of the D and G band differ only slightly. D/G ratios which are used to indicate the degree of disorder of the carbon frame are close: 0.99 for 1 keV, 0.98 for 2.5 keV, and 0.95 for 5 keV. The absence of any noticeable difference can be attributed to the fact that chemical changes induced by the ion beam are localized to the surface. The Raman signal is collected from bigger depth and it is thus dominated by the bulk properties of the paper.

For the process of surface reduction, we propose a mechanism based on localized thermal gradient caused by Ar^+ ion beam irradiation. In another words, as the Ar^+ ions penetrate the surface of the foil, they dissipate energy. This leads, according to ions energy, to local heating of GO, subsequently followed by a decomposition of oxygen functionalities. This is well documented by detection of CO_2, CO, and H_2O by mass spectrometry during the irradiation procedure. Additionally, under high vacuum conditions, the decomposition of oxygen functional groups is accelerated and higher C/O ratio achieved. Nonetheless, some differences compared to thermal reduction still remain. One example is methyl radical which can exist only in high vacuum. Its presence together with hydrogen molecules and nitrogen atoms well documents partial etching of the GO foil surface that takes place during Ar^+ irradiation. The fact that oxygen has larger cross-section for Ar^+ ions than carbon, in combination with thermal liability of oxygen functionalities, suggests that oxygen is released from the GO foil surface and graphene with high C/O ratio is formed.

3. Conclusion

We have successfully prepared highly reduced graphene papers with C/O ratio higher than 100 on the surface and 40 in bulk material. Such graphene papers show an excellent conductivity. The beam irradiation process was monitored in time by mass spectroscopy and X-ray photoelectron spectroscopy. We found out that molecules such as CO, CO_2, H_2O, as well as several complex organic molecules, are evolved during irradiation. The presence of hydrocarbon fragments leads us to believe that partial etching also takes place. Chemical changes both at the surface and in the depth of several nm reveal gradual reduction for all energies of the ion beam (1, 2.5, and 5 keV). However, energy of 1 keV is not enough to achieve full removal of the oxygen groups. Higher beam energies of 2.5 and 5 keV provided highly reduced surface which was proved by extremely high C/O ratio with oxygen free graphene surface. High conductivity of formed graphene was confirmed by the spreading resistance microscopy measurements. The increase of the number of C = C bonds and restoration of graphene structure are factors prevailingly responsible for this behavior. After the irradiation, the concentration of C–C/C–H bonds also increases which is probably caused by the reaction of reduced graphene at the surface with byproducts of the reduction.

No observable changes were detected in the surface morphology or structure. The reduction is localized to the surface and to the depth of several nm into the structure. Bulk properties of the material remain the same after the reduction.

We presented a simple and successful method for preparing compact graphene paper from GO papers without compromising other properties, such as thermal conductivity, thermal stability, tensile strength and Young's modulus, during the process. The Ar^+ ion beam with energy of 5 keV was sufficient to reduce the surface of GO paper and to obtain electrically conductive surface with Ohmic behavior and oxygen free surface of graphene. The described procedure is easy to conduct and has potential application in microelectronics and sensor devices.

4. Experimental Section

Graphite oxide was prepared, similarly to Hummers method, from pure graphite microparticles (2–15 μm, 99.9995%, from Alfa Aesar).[21] Sulfuric acid (98%), potassium permanganate (98%), sodium nitrate (99%), hydrogen peroxide (30%) and barium nitrate (99.5%) were obtained from Penta, Czech Republic. Argon of 99.999% purity was obtained from SIAD, Czech Republic.

5 g of graphite and 2.5 g of sodium nitrate were stirred with 115 mL of concentrated sulphuric acid. Then the mixture was cooled to 0 °C and, while vigorously stirred, 15 g of potassium permanganate was added over a period of two hours. In the subsequent four hours, the reaction mixture was allowed to reach the room temperature before being heated to 35 °C for 30 min. Afterwards, the reaction mixture was poured into a flask containing 250 mL of deionized water and heated to 70 °C for 15 min. The mixture was then poured into 1 dm^3 of deionized water. The unreacted potassium permanganate and manganese dioxide were removed by the addition of 3% hydrogen peroxide. The reaction mixture was allowed to settle and decanted. The obtained graphite oxide was purified by a repeated centrifugation and redispersing in deionized water until a negative reaction on sulphate ion (with $Ba(NO_3)_2$) was achieved. Pure GO was dispersed into distilled water in concentration of 5 mg dm^{-3}, spilled on the polished stainless steel plate and dried in a vacuum dryer at 50 °C. The produced film was peeled off and dried in a vacuum dryer for the next 2 hours.

ISE 100 ion gun from Omicron NanoTechnology was used for Ar^+ beam generation. The emission current was set to 1 mA. The surface of GO paper was irradiated by Ar^+ ions of various energies (1 keV, 2.5 keV, and 5 keV) in the preparation chamber. The beam current for beam energies of 1 keV, 2.5 keV, and 5 keV was 48 μA, 50 μA, and 48 μA, respectively. Diameter of the ion beam was 10 mm, therefore the exposed area of the GO paper was about 79 mm^2 and the current density of the ion beam was 61 μA cm^{-2}, 63 μA cm^{-2}, 61 μA cm^{-2} for 1 keV, 2.5 keV, and 5 keV, respectively. The irradiation was performed for up to 20 minutes in a preparation chamber under pressure of 2.0×10^{-3} Pa.

High resolution X-ray photoelectron spectroscopy (XPS) was performed with an ESCAProbeP (Omicron Nanotechnology Ltd, Germany) spectrometer using a monochromatic aluminum X-ray radiation source (1486.7 eV). The XPS spectra were acquired during the irradiation procedure. Angle resolved XPS was done in the measurement chamber perpendicular to the surface and under 10° to the surface plane in order to investigate surface properties of GO and deep profiles for the C/O ratio and carbon bonding characteristics. The high resolution XPS spectra were measured for C 1s and O 1s. To study the gas evolved during irradiation, the Ar^+ ion gun was used in the analysis chamber. These experiments were performed with 5 keV Ar^+ ions. Data were acquired by a quadrupole mass spectrometer (1–100 AMU) connected directly to the measurement chamber. During the irradiation by Ar^+ ions an increase of partial pressure of species originating from exfoliation procedure was observed (7.4×10^{-8} Pa).

The morphology was studied by atomic force microscopy (AFM) on NT-MTD Ntegra Spectra from NT-MDT in a tapping mode with Si tips under ambient condition with scan rate of 1 Hz and 512 scan lines. The conductivity and I-V characteristics were measured in a contact mode using Pt coated silicon tip (resonant frequency 30 kHz, force constant 0.01–0.5 N m^{-1}). The resistivity mapping was performed by scanning spreading resistance microscopy (SSRM) using the same device and same tips. The I-V curves were measured in the range of bias voltage ±6 V between the tip and the sample holder.

The surface resistivity of the Ar^+ irradiated area was measured by the standard four-probe technique using the Van der Pauw method. Graphene paper was cut into 5 mm × 5 mm squares and contacted in the corners by Pelco colloidal silver liquid from Ted Pella, Inc. Measurements were performed with a Keithley 6220 precision current source and an Agilent 34970A data acquisition/ switch unit. The measuring current was set to 0.1 mA.

Thermal stability of graphene and GO papers was analyzed by simultaneous thermal analysis (STA) on STA PT 1600 apparatus from Linseis Messgeraete GmbH. Samples were heated in a dynamic air atmosphere (50 mL min^{-1}) with a heating rate 10 °C min^{-1} from room temperature to 800 °C. Through plane thermal conductivity was determined using laser flash analysis (LFA) with pulse Nd:YAG laser from Linseis Messgeraete GmbH.

Mechanical strength was tested on Instron Universal Testing Machine 3365. Length of the crack was determined from SEM images.

The morphology of graphite oxide foil before and after irradiation with Ar^+ ions was observed by scanning electron microscopy using Tescan Lyra dual beam microscope with an FEG electron source. The observation was performed under the accelerating voltage of 10 kV. Powder sample was placed on a carbon conductive tape before measurement.

An inVia Raman microscope (Renishaw, England) in backscattering geometry with CCD detector was used for Raman spectroscopy. DPSS laser (532 nm, 50 mW) with 50× magnification objective was used for excitation of the sample. The instrument was calibrated with a silicon reference which gives a peak position at 520 cm^{-1} and a resolution of less than 1 cm^{-1}.

Supporting Information

Supporting Information is available from the Wiley Online Library or from the author.

Acknowledgements

This research was supported by a Specific University Research grant, MSMT No 20/2014, Czech Republic. M.P. acknowledges Tier 2 grant (MOE2013-T2–1–056; ARC 35/13) from Ministry of Education, Singapore.

Received: December 26, 2013
Revised: March 9, 2014
Published online: April 29, 2014

[1] W. Hu, Ch. Peng, W. Luo, M. Lv, X. Li, D. Li, Q. Huang, Ch. Fan, *ACS Nano* **2010**, *4*, 4317.
[2] J. K. Lee, K. B. Smith, C. M. Hayner, H. H. Kung, *Chem. Commun.* **2010**, *46*, 2025.
[3] L. Ji, Z. Tan, T. Kuykendall, E. J. An, Y. Fu, V. Battaglia, Y. Zhang, *Energy Environ. Sci.* **2011**, *4*, 3611.
[4] L. Ji, Z. Tan, T. Kuykendall, S. Aloni, S. Xun, E. Lin, V. Battaglia, Y. Zhang, *Phys. Chem. Chem. Phys.* **2011**, *13*, 7170.
[5] L. Ji, H. Zheng, A. Ismach, Z. Tan, S. Xun, E. Lin, V. Battaglia, V. Srinivasan, Y. Zhang, *Nano Energy* **2011**, *1*, 164.
[6] L. Ji, H. L. Xin, T. R. Kuykendall, S.-L. Wu, H. Zheng, M. Rao, E. J. Cairns, V. Battaglia, Y. Zhang, *Phys. Chem. Chem. Phys.* **2012**, *14*, 6981.
[7] D. A. Dikin, S. Stankovich, E. J. Zimney, R. D. Piner, G. H. B. Dommet, G. Evmenenko, S. T. Nguyen, R. S. Ruoff, *Nat. Lett.* **2007**, *448*, 457.
[8] Z. Wei, D. E. Barlow, P. E. Sheehan, *Nano Lett.* **2008**, *8*, 3141.
[9] X. Li, G. Zhang, X. Bai, X. Sun, X. Wang, E. Wang, H. Dai, *Nat. Nanotechnol.* **2008**, *3*, 538.
[10] K. S. Kim, Y. Zhao, H. Jang, S. Y. Lee, J. M. Kim, K. S. Kim, J. H. Ahn, P. Kim, J. Y. Choi, B. H. Hong, *Nature* **2009**, *457*, 706.
[11] Ch. Chen, Q.-H. Yang, Y. Yang, W. Lv, Y. Wen, P.-X. Hou, M. Wang, H.-M. Cheng, *Adv. Mater.* **2009**, *21*, 3007.
[12] S. Park, K.-S. Lee, G. Bozoklu, W. Cai, S. T. Nguyen, R. S. Ruoff, *ACS Nano* **2008**, *2*, 572.
[13] G. Eda, G. Fanchini, M. Chhowalla, *Nat. Nanotechnol.* **2008**, *3*, 270.
[14] J. T. Robinson, M. Zalalutdinov, J. W. Baldwin, E. S. Snow, Z. Wei, P. Sheehan, B. H. Houston, *Nano Lett.* **2008**, *8*, 3441.
[15] S. Park, D. A. Dikin, S. T. Nguyen, R. S. Ruoff, *Phys. Chem. Lett. C* **2009**, *113*, 15801.
[16] D. Yang, A. Velamakanni, G. Bozoklu, S. Park, M. Stoller, R. D. Piner, S. Stankovich, I. Jung, D. A. Field, C. A. Ventrice Jr., R. S. Ruoff, *Carbon* **2009**, *47*, 145.
[17] S. Park, J. An, I. Jung, R. D. Piner, S. J. An, X. Li, A. Velemakanni, R. S. Ruoff, *Nano Lett.* **2009**, *9*, 1593.
[18] H. Chen, M. B. Muller, K. J. Gilmore, G. G. Wallace, D. Li, *Adv. Mater.* **2008**, *20*, 3557.
[19] S. Park, J. An, R. D. Piner, I. Jung, D. Yang, A. Velemakanni, S. T. Nguyen, R. S. Ruoff, *Chem. Mater.* **2008**, *20*, 6592.
[20] O. C. Compton, D. A. Dikin, K. W. Putz, L. C. Brinson, S. T. Nguyen, *Adv. Mater.* **2010**, *22*, 892.
[21] W. S. Hummers, R. E. Offeman, *J. Am. Chem. Soc.* **1958**, *80*, 1339.